

CONTRAST-ENHANCED ULTRASONOGRAPHY FOR CHARACTERIZATION OF CANINE FOCAL LIVER LESIONS

KENSUKE NAKAMURA, SATOSHI TAKAGI, NOBORU SASAKI, WICKRAMASEKARA RAJAPAKSHAGE BANDULA KUMARA, MASAHIRO MURAKAMI, HIROSHI OHTA, MASAHIRO YAMASAKI, MITSUYOSHI TAKIGUCHI

In six normal beagles and 27 dogs with spontaneous focal or multifocal liver lesions, contrast-enhanced ultrasonography using Sonazoid[®] was performed. Sonazoid[®] is a newly developed second-generation contrast agent with the ability to be used for real-time contrast imaging along with parenchymal imaging. An appropriate protocol for the evaluation of all three phases (arterial, portal, and parenchymal) was established based on the results for normal beagles. By evaluation of the echogenicity of hepatic nodules during the arterial and parenchymal phases it was possible to differentiate malignant tumors from benign nodules with very high accuracy. In 15 of 16 dogs diagnosed as malignant tumors, nodules were clearly hypoechoic to the surrounding normal liver during the parenchymal phase. Additionally, malignant tumors had different echogenicity compared with the surrounding normal liver during the arterial phase in 14 of 15 dogs. In the portal phase, there were no characteristic findings. Contrast-enhanced ultrasonography with Sonazoid[®] appears to improve the characterization of canine focal and multifocal hepatic lesions. *Veterinary Radiology & Ultrasound, Vol. 51, No. 1, 2010, pp 79–85.*

Key words: contrast, dog, liver, Sonazoid[®], tumor, ultrasonography.

Introduction

CONVENTIONAL ULTRASONOGRAPHY HAS low specificity for characterizing focal liver lesions.^{1,2} For example, tumor vascularity is important for tumor characterization, but this can be done more accurately with computed tomography or magnetic resonance imaging.^{3,4}

Recent advances in ultrasonographic contrast agents have led to sonographic improvements in assessing tumor vascularity.⁵ In addition to vascular imaging, Levovist[®], one of the first-generation contrast agents, was also phagocytized by Kupffer cells, allowing for parenchymal imaging after the vascular phase.^{6,7} This parenchymal imaging improves the detection and delineation of focal tumors, given that malignant tumors have little or no reticuloendothelial system and appear as hypoechoic defects.^{8–12} However, Levovist bubbles are easily collapsed by ultrasound emission because of their fragility. Therefore, Levovist-enhanced ultrasonographic images can be obtained only within a short window of time in the vascular phase, and Kupffer imaging can only be performed during a single scan of the liver.

Second-generation contrast agents, comprised of harder shells, allow continuous real-time evaluation of progressive contrast enhancement of the macro- and microvasculature of the normal liver parenchyma and focal liver lesions during the arterial, portal, and late vascular phases with low acoustic power (a low mechanical index [MI]).¹³ The evaluation of the arterial, portal, and late vascular phases with second-generation contrast agents allows differential diagnosis of focal liver lesions with high accuracy.^{14–16} The new contrast agent Sonazoid[®] is a suitable agent for parenchymal imaging because it is one of the few second-generation contrast agents phagocytized by Kupffer cells.^{17–19} Contrast-enhanced ultrasonography with Sonazoid[®] allows an accurate diagnosis of hepatic tumors.^{20–22}

In veterinary medicine, contrast-enhanced ultrasonography is performed for the liver, spleen, and kidney.^{23–34} The liver is the most common organ investigated.^{23–27,31,33,34} The utility of Sonazoid[®], however, has been uncertain in veterinary medicine because most contrast agents used in these studies were blood-pool agents^{23–25,27–30,34} or first-generation agents.²⁶ There are only two reports of the use of Sonazoid[®]-enhanced ultrasonography for canine liver.^{31,33} Thus, the purpose of this study was to determine the appropriate timing for the arterial, portal, and parenchymal phases in the normal canine liver and to evaluate the usefulness of these imaging methods with Sonazoid[®] in clinical patients with hepatic nodules.

From the Laboratory of Veterinary Internal Medicine, (Nakamura, Sasaki, Bandula Kumara, Murakami, Ohta, Yamasaki, Takiguchi) and Laboratory of Veterinary Surgery, Department of Veterinary Clinical Sciences, Graduate School of Veterinary Medicine, Hokkaido University, N18 W9 Sapporo, Hokkaido 060-0818, Japan (Takagi).

Address correspondence and reprint requests to Dr. Mitsuyoshi Takiguchi, at the above address. E-mail: mtaki@vetmed.hokudai.ac.jp

Received February 3, 2009; accepted for publication July 16, 2009.

doi: 10.1111/j.1740-8261.2009.01627.x

Materials and Methods

Six adult laboratory beagles weighing between 7.5 and 14.5 kg were studied. Each dog was healthy based on physical examination and laboratory data. No focal or diffuse hepatic abnormality was noted in any dog on ultrasonographic evaluation. All procedures involving animals were approved by the Hokkaido University Animal Care and Use Committee.

An ultrasound scanner* with a 5–11 MHz broadband linear probe† suitable for pulse subtraction imaging was used. The mechanical index was set at 0.2 MI to minimize microbubble destruction. The B-mode gain was 90 dB. Images were recorded for off-line analysis.

We estimated that a Sonazoid‡ dose of 0.12 µl microbubbles/kg would be suitable as a clinical dose, in accordance with the manufacturer's instructions and data from rabbits in which the liver parenchyma was enhanced at doses ranging from 0.045 to 0.315 µl microbubbles/kg.¹⁷ We injected a single bolus of the contrast agent in the cephalic vein through a 22-G catheter. Beagles were not sedated. The cranial abdomen was shaved, and the dog was in dorsal recumbency. The liver and portal vein were scanned in one image. Intermittent imaging for several seconds at 0, 1, 2, 3, 4, 5, 6, 7, 8, 9, 10, 15, and 30 min after injection was performed so as to minimize microbubble destruction.

For quantitative analysis, individual ultrasound images were acquired using a video frame grabber. An off-line image analysis system was used for calculating signal intensity (ImageJ, US National Institutes of Health, <http://rsb.info.nih.gov/ij/>). In this system, the gray-scale level ranged from a mean pixel value of 0 to 255. Signal intensity was obtained for the liver parenchyma and portal vein.

Statistical analysis was performed using Dunnett's multiple comparison tests to evaluate the difference between pre- and postinjection values of each region and by Student's *t*-test to evaluate the difference between the liver parenchyma and portal vein at the same time. A *P* value of <0.05 was considered to be significant. Statistical analysis was performed with a standard computer software program.§

Twenty-eight lesions in 27 canine patients were evaluated with Sonazoid‡. Inclusion criteria were sonographic evidence of hepatic nodules and histologic or cytologic diagnosis of a liver lesion. An ultrasound scanner* with a 5–11 MHz broadband linear probe (PLT-704 AT) or a 3.75 MHz convex probe¶ suitable for pulse subtraction imaging was selected according to the depth and size of the

lesion. A single focal zone was placed in the deepest part of the lesion. The mechanical index was set at 0.2 MI to minimize microbubble destruction. The gain was set so that few signals from the underlying liver parenchyma were present. The images were recorded for off-line analysis. Dogs were not sedated. The cranial abdomen was shaved and the dog was in dorsal recumbency. Sonazoid‡ (0.12 µl microbubbles/kg) was injected in the cephalic vein via an intravenous catheter while scanning the lesion. Real-time imaging was performed during the arterial, portal, and parenchymal phases. For arterial and portal imaging, we scanned the lesion continuously from 0 to 1 min after injection. Then, the parenchymal imaging was obtained at least 7 min after injection. The timing of all three phases was defined based on the results from the normal beagle dogs. The echogenicity of the liver lesion was evaluated as hypoechoic, isoechoic, or hyperechoic relative to the surrounding normal liver.

Individual ultrasound images were acquired using a video frame grabber. The relationship between the echogenicity and malignancy of the lesion was analyzed using a two-tailed Fisher's exact test with a level of significance of *P* < 0.01. Statistical analysis was performed with a standard computer software program.§

Results

In the beagle dogs, the hepatic arteries were enhanced immediately after injection but the enhancement dispersed rapidly. After arterial enhancement, the portal vein became enhanced followed by the parenchyma. The mean, ± standard deviation, pixel value of the parenchyma and portal vein were 65.6 ± 13.2 and 53.1 ± 13.4, respectively. The mean pixel value of the portal vein (175.0 ± 25.6 MPV) was higher than that of the parenchyma (151.2 ± 13.9 MPV) until 1 min after injection (*P* < 0.05) (Fig. 1). The contrast effect decreased abruptly and the mean pixel value at 7 min after injection (63.3 ± 10.2) was not significantly different from baseline (Fig. 1). Contrast enhancement of the parenchyma decreased only slightly (*P* < 0.05) with a mean pixel value of 128.7 ± 15.6 being maintained up to 30 min. Thus, the optimal time for parenchymal imaging is from 7 to 30 min after injection and the optimal time for portal vein imaging is 1 min after injection. The timing of the arterial phase could not be defined based on the change of echogenicity of the hepatic arteries because they were too thin to be assessed. Thus we defined the arterial phase as the moment when the echogenicity of the portal vein began to rise.³⁵

Of the 27 clinical patients with 28 hepatic nodules, five dogs had a benign nodule, 21 dogs had a malignant nodule, and one dog had both benign and malignant nodules. Histologic examination was available for 20 lesions; five were benign nodular hyperplasia and 15 were malignant.

*Aplio XG, Toshiba Medical Systems, Tochigi, Japan.

†PLT-704 AT, Toshiba Medical Systems.

‡Daiichi-Sankyo, Tokyo, Japan.

§StatMate®, ATMS, Tokyo, Japan.

¶PSK-375 BT, Toshiba Medical Systems.

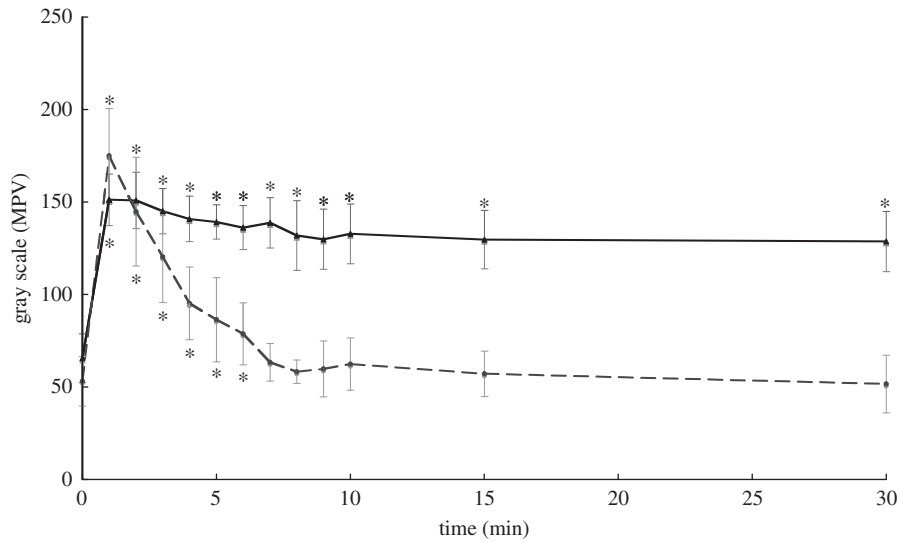


FIG. 1. Time-intensity curves of liver parenchyma (solid line) and portal vein (dotted line) (0 to 30 min after injection of Sonazoid®) in six normal beagles. Bars = standard error of the mean. *Significantly ($P < 0.05$) different from the preinjection values (Dunnett's test).

The 15 malignancies were comprised of 11 hepatocellular carcinomas, one combined hepatocellular and cholangiocellular carcinoma, one carcinoid, one hemangiosarcoma, and one osteosarcoma. Needle aspirates were taken with ultrasound guidance in the other eight lesions with six suspected hemangiosarcomas, one lymphoma, and one nodular hyperplasia. Finally, 16 lesions were diagnosed as malignant tumors, and six lesions were diagnosed as benign lesions (Table 1).

All six benign lesions were isoechoic to the surrounding normal liver during the parenchymal phase. On the other hand, 15 of the 16 lesions with a confirmed diagnosis of malignancy were hypoechoic (Fig. 2). This finding was significantly ($P < 0.01$) correlated with malignancy with an

accuracy of 95.5% (95% confidence interval [CI], 79.5–95.5%), a sensitivity of 93.8% (95% CI, 82.8–93.8%), a specificity of 100% (95% CI, 70.7–100%), a positive predictive value of 100% (95% CI, 88.3–100%), and a negative predictive value of 85.7% (95% CI, 60.6–85.7%). Additionally, five of the six benign lesions were isoechoic during the arterial phase. Among the 15 malignant lesions, conversely, only one lesion was isoechoic, 11 lesions were hyperechoic, and three lesions were hypoechoic. Hyper-echogenicity or hypoechogenicity at the arterial phase was also significantly related to malignancy ($P < 0.01$) with an accuracy of 90.5% (95% CI, 72.7–97.3%), a sensitivity of 93.3% (95% CI, 80.9–98.1%), a specificity of 83.3% (95% CI, 52.2–95.3%), a positive predictive value of 93.3% (95%

TABLE 1. Histological Type and Contrast Enhanced Ultrasonographic Appearance of the Liver Lesions of Dogs in this Study

Lesion	Mean Size (Range) (cm)	Echogenicity of the Liver Lesions Compared with the Surrounding Normal Liver Parenchyma		
		Arterial Phase	Portal Phase	Parenchymal Phase
Malignancy (n = 22)				
Epithelial tumor (n = 13)				
Hepatocellular carcinoma (n = 11)	4.2 (2.0–8.2)	Hyper (n = 9), Iso (n = 1) Hypo (n = 1)	Hyper (n = 1), Iso (n = 6), Hypo (n = 1), Mix (n = 3)	Hypo (n = 10), Iso (n = 1)
Combined hepatocellular cholangiocellular carcinoma (n = 1)	1.3	Hyper (n = 1)	Mix (n = 1)	Hypo (n = 1)
Carcinoid (n = 1)	Multiple (0.5–0.7)	Hyper (n = 1)	Hypo (n = 1)	Hypo (n = 1)
Mesenchymal tumor (n = 8)				
Hemangiosarcoma (n = 1)	1.7	Hypo (n = 1)	Hypo (n = 1)	Hypo (n = 1)
Osteosarcoma (n = 1)	2.5	Hypo (n = 1)	Hypo (n = 1)	Hypo (n = 1)
Hemangiosarcoma suspected (n = 6)	4.3 (1.8–8.0)	Hypo (n = 6)	Hypo (n = 6)	Hypo (n = 6)
Hematopoietic tumor (n = 1)				
Lymphoma (n = 1)	1.8	Not examined (n = 1)	Not examined (n = 1)	Hypo (n = 1)
Benignancy (n = 6)				
Nodular hyperplasia (n = 6)	1.5 (0.5–3.3)	Iso (n = 5), Hyper (n = 1)	Iso (n = 5), Hyper (n = 1)	Iso (n = 6)

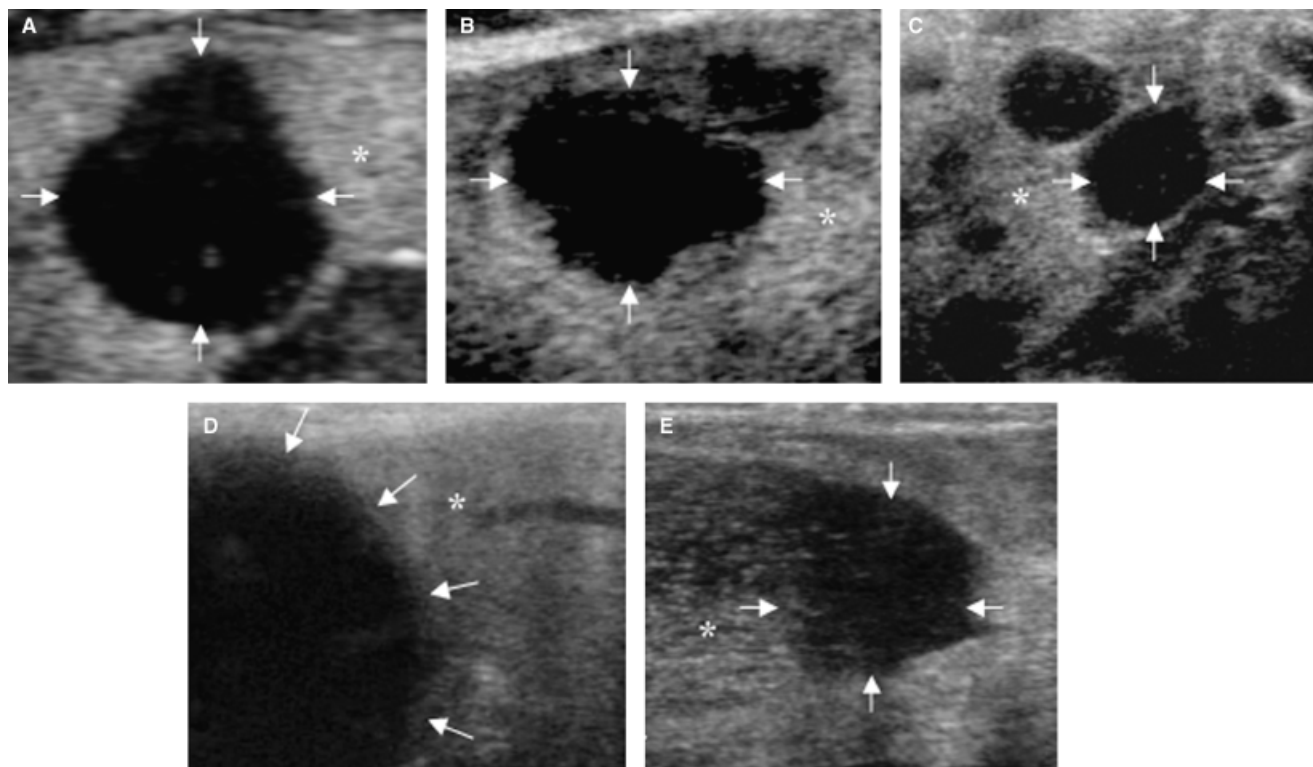


FIG. 2. Ultrasound images of contrast enhancement during the parenchymal phase of hepatic malignant tumors; (A) hepatocellular carcinoma, (B) combined hepatocellular cholangiocellular carcinoma, (C) carcinoid, (D) hepatic osteosarcoma, (E) lymphoma. All lesions had clear contrast defects (arrows) compared with surrounding normal parenchyma (*).

CI, 80.9–98.1%), and a negative predictive value of 83.3% (95% CI, 52.2–95.3%). In the portal phase, there were no characteristic findings.

The benign nodules were all nodular hyperplasia ($n=6$). Among them, five were diagnosed histologically and one cytologically. In the arterial phase, five of the nodular hyperplasias were isoechoic to the surrounding liver (Fig. 3A and

B). In the portal phase, five remained isoechoic and one became hyperechoic. In the parenchymal phase, all six were isoechoic, defined as contrast enhancement (Fig. 3C).

Hepatocellular carcinoma ($n=11$) was the most common malignant tumor. Immediately after injection of Sonoazoid[®], the branching vasculature became enhanced momentarily in nine of these 11 dogs (Fig. 4A). In nine

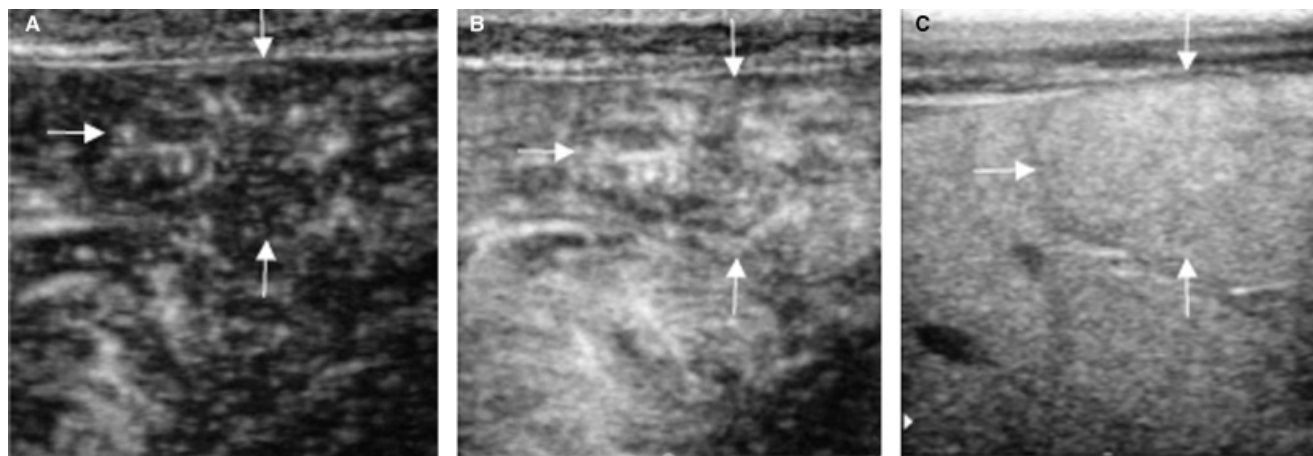


FIG. 3. Ultrasound images of contrast enhancement of nodular hyperplasia. (A) The vasculature pattern in the lesion was not different from the surrounding normal parenchyma. (B) During the arterial phase, the lesion was isoechoic (arrows) compared with the surrounding normal lesion. (C) During the parenchymal phase, the lesion was isoechoic (arrows).

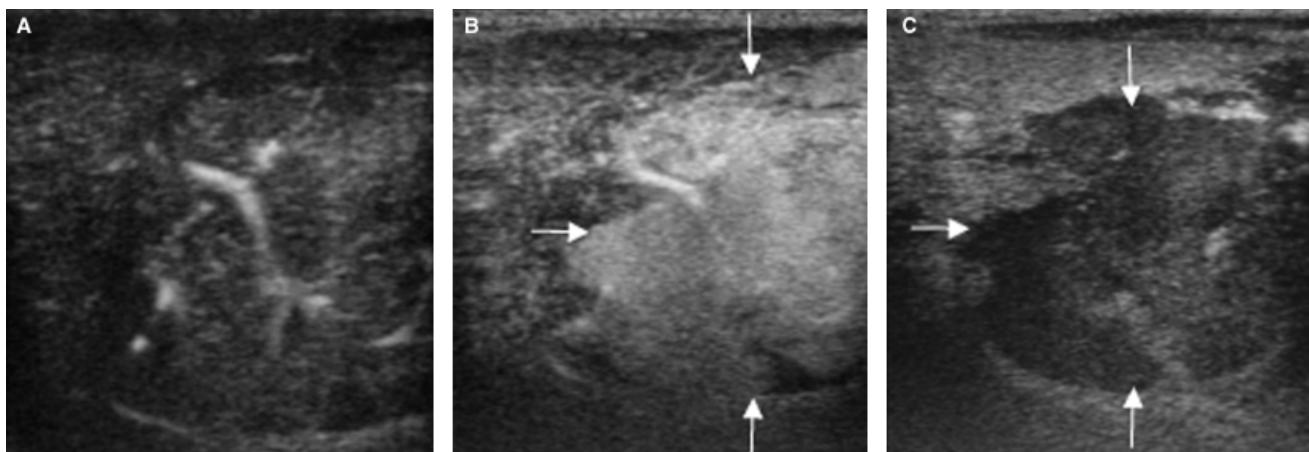


FIG. 4. Ultrasound images of contrast enhancement of hepatocellular carcinoma. (A) The branching vasculature was enhanced immediately after injection of Sonazoid[®]. (B) During the arterial phase, the lesion was hyperechoic (arrows) compared with the surrounding normal parenchyma. (C) During the parenchymal phase, the lesion was hypoechoic (arrows).

of the 11 dogs, nodules were hyperechoic to the surrounding normal liver during the arterial phase (Fig. 4B). In one dog, the nodule was hypoechoic to the surrounding normal liver during the arterial phase. In the portal phase, there was no characteristic finding. In the parenchymal phase, 10 of the 11 nodules were hypoechoic (Figs. 2A and 4C). Only one dog had an isoechoic nodule, defined as contrast enhancement.

One dog had a combined hepatocellular and cholangiocellular carcinoma. The nodule was hyperechoic during the arterial phase, then became hypoechoic during the parenchymal phase (Fig. 2B). One dog had a carcinoid. There were multiple small nodules in the liver in this patient. These nodules were hyperechoic during the arterial phase, then hypoechoic in the parenchymal phase (Fig. 2C). One dog had histologically proven hemangiosarcoma. The nodule was hypoechoic during all phases (Fig. 5).

Hemangiosarcoma was suspected in six other dogs based on cytology; none of these nodules were enhanced during any phase. One dog had a hepatic osteosarcoma. This lesion was hypoechoic to the surrounding normal liver during all three phases (Fig. 2D). One dog had lymphoma and, using conventional ultrasonography, some nodules could not be recognized. Evaluation of the vascular phase was not possible because of patient motion. During the parenchymal phase, multiple hypoechoic nodules were detected (Fig. 2E).

Discussion

Our goal was to assess the clinical utility of Sonazoid[®]-enhanced ultrasonography for characterization of canine focal liver lesions. Our findings suggest that Sonazoid[®]-enhanced ultrasonography has value in differentiating

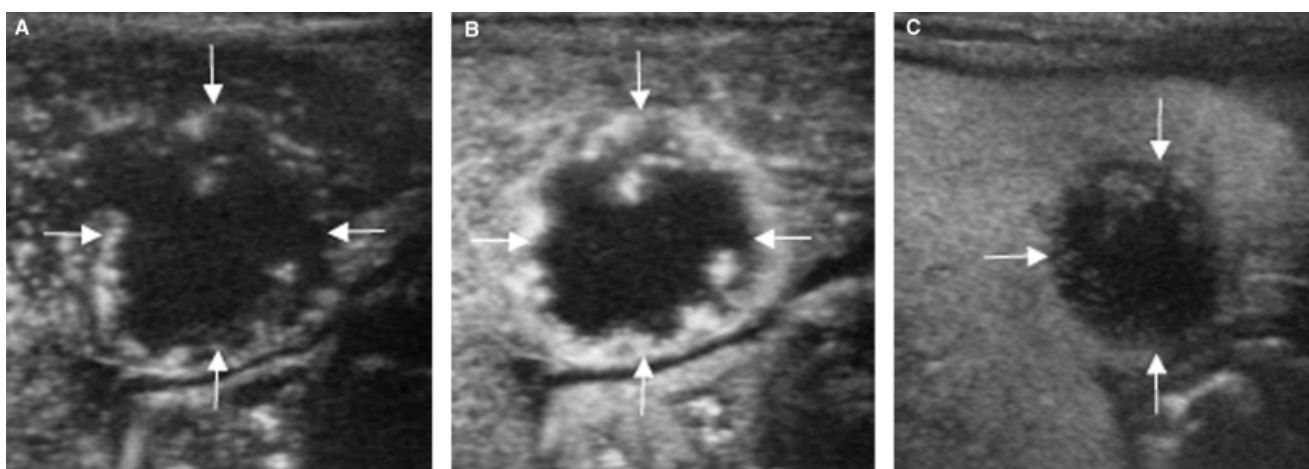


FIG. 5. Ultrasound images of contrast enhancement of hemangiosarcoma. (A) The nodule was not enhanced immediately after injection of Sonazoid[®]. (B) During the arterial phase, the lesion was hypoechoic (arrows) compared with the surrounding normal parenchyma. (C) During the parenchymal phase, the lesion was hypoechoic (arrows).

between malignant tumors and benign nodules with high accuracy.

In normal dogs, Sonazoid[®] led to enhanced signal from the portal vein and hepatic parenchyma immediately after injection. Uniform contrast enhancement was maintained for at least 30 min in the liver parenchyma. The signal intensity from the portal vein was the highest at 1 min after injection and then enhancement of the portal vein decreased gradually and disappeared at 7 min after injection. On the basis of these findings, we defined the portal phase as 1 min after injection and the parenchymal phase as 7–30 min after injection. Hepatic arteries were too thin to evaluate. However, the time at which echogenicity of the portal vein begins to rise is within the arterial phase.³⁵ Thus we defined the arterial phase as the moment when the echogenicity of the portal vein started to rise.

In clinical patients, malignant nodules were clearly filling defects following Sonazoid[®] injection. This agrees with findings from humans.^{20–22} Parenchymal enhancement in rat liver following Sonazoid[®] injection is due to the distribution of the microbubbles in the Kupffer cells and not in the sinusoids.¹⁷ The filling defect during the parenchymal phase created by the malignant nodule is then due to a decrease in the number of Kupffer cells.

Our findings with regard to hepatocellular carcinoma are not in complete agreement with prior work in the dog.³³ In that study, the presence of an incomplete, irregular, or partial defect during the parenchymal phase was characteristic of hepatocellular carcinoma compared with other malignant tumors.³³ This was hypothesized to be due to residual Kupffer cells in hepatocellular carcinoma nodules. In our study, no hepatocellular carcinoma was heteroechoic and most were homogeneously hypoechoic, similar to other malignant tumors. On the other hand, one hepatocellular carcinoma was isoechoic, supporting the presence of large numbers of Kupffer cells in that patient. These findings suggest that the number of Kupffer cells in canine hepatocellular carcinoma differs among patients. In humans, it is indicated that the echogenicity during the parenchymal phase changes from isoechoic to hypoechoic through heteroechoic with progression of histologic grades.²² Additionally, some studies revealed that Kupffer cells were present in human early stage and well-differen-

tiated hepatocellular carcinoma.^{36–38} Further studies are needed to investigate the relationship between the histologic grade of canine hepatocellular carcinoma and Kupffer cells.

Arterial imaging was also useful to differentiate between malignant and benign lesions. In the present study, nodular hyperplasia was isoechoic and hepatocellular carcinoma was hyperechoic during the arterial phase. These findings agreed with those of previous studies.^{24,33} On the other hand, all hemangiosarcomas were hypoechoic during all three phases. This concurred with findings using other ultrasound contrast agents^{24,34} and contrast-enhanced computed tomography.³⁹ In addition to echogenicity, the vasculature patterns during the arterial phase are used to characterize human²⁰ and dog³³ focal liver lesions. In the present study, hepatocellular carcinoma had a branching vasculature pattern. This agreed with the finding for humans²⁰, but was incongruent with the finding for dogs.³⁸ The reason for this difference is uncertain. However, it is quite difficult to evaluate the vasculature pattern accurately because of patient motion and the quite short duration of vasculature enhancement in dogs. Therefore, the vasculature pattern of the canine focal liver lesion should not be overestimated.

There were some limitations in this study. First, the number of patients with benign nodules was small. Therefore, there were large confidence intervals for the specificity and negative predictive value for differentiation between malignant and benign liver lesions. Second, only one hemangiosarcoma was diagnosed histologically. Third, the criteria for diagnosis were not applied prospectively. A prospective study is needed to confirm the accuracy for differential diagnosis of hepatic nodules.

In conclusion, Sonazoid[®]-enhanced ultrasonography according to the protocol established in this study can be used to differentiate canine hepatic malignant tumors and benign nodules with high accuracy. However, further study is needed to make a definite diagnosis based on the findings of Sonazoid[®]-enhanced ultrasonography.

ACKNOWLEDGMENT

We thank Toshiba Medical Systems for providing the ultrasound machine.

REFERENCES

1. Lamb CR. Abdominal ultrasonography in small animals: examination of the liver, spleen and pancreas. *J Small Anim Pract* 1990;31:5–14.
2. Cuccovillo A, Lamb CR. Cellular features of sonographic target lesions of the liver and spleen in 21 dogs and a cat. *Vet Radiol Ultrasound* 2002;43:275–278.
3. Shinmura R, Matsui O, Kadoya M, et al. Detection of hypervascular malignant foci in borderline lesions of hepatocellular carcinoma: comparison of dynamic multi-detector row CT, dynamic MR imaging and superparamagnetic iron oxide-enhanced MR imaging. *Eur Radiol* 2008;18:1918–1924.
4. Clifford CA, Pretorius ES, Weisse C, et al. Magnetic resonance imaging of focal splenic and hepatic lesions in the dog. *J Vet Intern Med* 2004;18:330–338.
5. Leen E. The role of contrast-enhanced ultrasound in the characterization of focal liver lesions. *Eur Radiol* 2001;11(Suppl 3):E27–E34.
6. Yanagisawa K, Moriyasu F, Miyahara T, Yuki M, Iijima H. Phagocytosis of ultrasound contrast agent microbubbles by Kupffer cells. *Ultrasound Med Biol* 2007;33:318–325.
7. Blomley MJK, Albrecht T, Cosgrove DO, et al. Stimulated acoustic emission to image a late liver and spleen-specific phase of Levovist in normal

volunteers and patients with and without liver disease. *Ultrasound Med Biol* 1999;25:1341–1352.

8. Harvey CJ, Blomley MJ, Eckersley RJ, et al. Hepatic malignancies: improved detection with pulse-inversion US in late phase of enhancement with SH U 508A—early experience. *Radiology* 2000;216:903–908.

9. Rabenandrasana HA, Furukawa A, Furuichi K, Yamasaki M, Takahashi M, Murata K. Comparison between tissue harmonic imaging and liver-specific late-phase contrast-enhanced pulse-inversion imaging in the detection of hepatocellular carcinoma and liver metastasis. *Radiat Med* 2004;22:90–97.

10. Heckemann RA, Cosgrove DO, Blomley MJ, Eckersley RJ, Harvey CJ, Mine Y. Liver lesions: intermittent second-harmonic gray-scale US can increase conspicuity with microbubble contrast material—early experience. *Radiology* 2000;216:592–596.

11. von Herbay A, Vogt C, Häussinger D. Late-phase pulse-inversion sonography using the contrast agent Levovist: differentiation between benign and malignant focal lesions of the liver. *Am J Roentgenol* 2002;179:1273–1279.

12. Bryant TH, Blomley MJ, Albrecht T, et al. Improved characterization of liver lesions with liver-phase uptake of liver-specific microbubbles: prospective multicenter study. *Radiology* 2004;232:799–809.

13. Nicolau C, Brú C. Focal liver lesions: evaluation with contrast-enhanced ultrasonography. *Abdom Imaging* 2004;29:348–359.

14. Nicolau C, Vilana R, Catalá V, et al. Importance of evaluating all vascular phases on contrast-enhanced sonography in the differentiation of benign from malignant focal liver lesions. *Am J Roentgenol* 2006;186:158–167.

15. von Herbay A, Vogt C, Willers R, Häussinger D. Real-time imaging with the sonographic contrast agent SonoVue: differentiation between benign and malignant hepatic lesions. *J Ultrasound Med* 2004;23:1557–1568.

16. Lencioni R, Piscaglia F, Bolondi L. Contrast-enhanced ultrasound in the diagnosis of hepatocellular carcinoma. *J Hepatol* 2008;48:848–857.

17. Watanabe R, Matsumura M, Chen CJ, Kaneda Y, Ishihara M, Fujimaki M. Gray-scale liver enhancement with Sonazoid (NC100100), a novel ultrasound contrast agent; detection of hepatic tumors in a rabbit model. *Biol Pharm Bull* 2003;26:1272–1277.

18. Watanabe R, Matsumura M, Chen CJ, Kaneda Y, Fujimaki M. Characterization of tumor imaging with microbubble-based ultrasound contrast agent, Sonazoid, in rabbit liver. *Biol Pharm Bull* 2005;28:972–977.

19. Watanabe R, Matsumura M, Munemasa T, Fujimaki M, Suematsu M. Mechanism of hepatic parenchyma-specific contrast of microbubble-based contrast agent for ultrasonography: microscopic studies in rat liver. *Invest Radiol* 2007;42:643–651.

20. Hatanaka K, Kudo M, Minami Y, et al. Differential diagnosis of hepatic tumors: value of contrast-enhanced harmonic sonography using the newly developed contrast agent, Sonazoid. *Intervirology* 2008;5:61–69.

21. Hatanaka K, Kudo M, Minami Y, Maekawa K. Sonazoid-enhanced ultrasonography for diagnosis of hepatic malignancies: comparison with contrast-enhanced CT. *Oncology* 2008;75(Suppl 1):42–47.

22. Inoue T, Kudo M, Hatanaka K, et al. Imaging of hepatocellular carcinoma: qualitative and quantitative analysis of postvascular phase contrast-enhanced ultrasonography with Sonazoid. Comparison with superparamagnetic iron oxide magnetic resonance images. *Oncology* 2008;75(Suppl 1):48–54.

23. Ziegler LE, O'Brien RT, Waller KR, Zagzebski JA. Quantitative contrast harmonic ultrasound imaging of normal canine liver. *Vet Radiol Ultrasound* 2003;44:451–454.

24. O'Brien RT, Iani M, Matheson J, Delaney F, Young K. Contrast harmonic ultrasound of spontaneous liver nodules in 32 dogs. *Vet Radiol Ultrasound* 2004;45:547–553.

25. Nyman HT, Kristensen AT, Kjelgaard-Hansen M, McEvoy FJ. Contrast-enhanced ultrasonography in normal canine liver. Evaluation of imaging and safety parameters. *Vet Radiol Ultrasound* 2005;46:243–250.

26. Kutara K, Asano K, Kito A, et al. Contrast harmonic imaging of canine hepatic tumors. *J Vet Med Sci* 2006;68:433–448.

27. O'Brien RT. Improved detection of metastatic hepatic hemangiosarcoma nodules with contrast ultrasound in three dogs. *Vet Radiol Ultrasound* 2007;48:146–148.

28. Ohlerth S, Ruefli E, Poirier V, Roos M, Kaser-Hotz B. Contrast harmonic imaging of the normal canine spleen. *Vet Radiol Ultrasound* 2007;48:451–456.

29. Waller KR, O'Brien RT, Zagzebski JA. Quantitative contrast ultrasound analysis of renal perfusion in normal dogs. *Vet Radiol Ultrasound* 2007;48:373–377.

30. Rossi F, Leone VF, Vignoli M, Laddaga E, Terragni R. Use of contrast-enhanced ultrasound for characterization of focal splenic lesions. *Vet Radiol Ultrasound* 2008;49:154–164.

31. Kanemoto H, Ohno K, Nakashima K, Takahashi M, Fujino Y, Tsujimoto H. Vascular and Kupffer imaging of canine liver and spleen using the new contrast agent Sonazoid. *J Vet Med Sci* 2008;70:1265–1268.

32. Nakamura K, Sasaki N, Yoshikawa M, et al. Quantitative contrast-enhanced ultrasonography of canine spleen. *Vet Radiol Ultrasound* 2009;50:104–108.

33. Kanemoto H, Ohno K, Nakashima K, et al. Characterization of canine focal liver lesions with contrast-enhanced ultrasound using a novel contrast agent—Sonazoid. *Vet Radiol Ultrasound* 2009;50:188–194.

34. Ivancić M, Long F, Seiler GS. Contrast harmonic ultrasonography of splenic masses and associated liver nodules in dogs. *J Am Vet Med Assoc* 2009;234:88–94.

35. Iijima H, Sasaki S, Moriyasu F, et al. Dynamic US contrast study of the liver: vascular and delayed parenchymal phase. *Hepatol Res* 2007;37:27–34.

36. Liu K, He X, Lei XZ, et al. Pathomorphological study on location and distribution of Kupffer cells in hepatocellular carcinoma. *World J Gastroenterol* 2003;9:1946–1949.

37. Tanaka M, Nakashima O, Wada Y, Kage M, Kojiro M. Pathomorphological study of Kupffer cells in hepatocellular carcinoma and hyperplastic nodular lesions in the liver. *Hepatology* 1996;24:807–812.

38. Inoue T, Kudo M, Maenishi O, et al. Value of liver parenchymal phase contrast-enhanced sonography to diagnose premalignant and borderline lesions and overt hepatocellular carcinoma. *Am J Roentgenol* 2009;192:698–705.

39. Fife WD, Samii VF, Drost WT, Mattoon JS, Hoshaw-Woodard S. Comparison between malignant and nonmalignant splenic masses in dogs using contrast-enhanced computed tomography. *Vet Radiol Ultrasound* 2004;45:289–297.